

EXPERT SELECTIONS IN MOE MODELS REVEAL (ALMOST) AS MUCH AS TEXT

Amir Nuriyev
MBZUAI

Gabriel Kulp
RAND, Oregon State University

ABSTRACT

We present a text-reconstruction attack on mixture-of-experts (MoE) language models that recovers tokens from expert selections alone. In MoE models, each token is routed to a subset of expert subnetworks; we show these routing decisions leak substantially more information than previously understood. Prior work using logistic regression achieves limited reconstruction; we show that a 3-layer MLP improves this to 63.1% top-1 accuracy, and that a transformer-based sequence decoder recovers 91.2% of tokens top-1 (94.8% top-10) on 32-token sequences from OpenWebText after training on 100M tokens. These results connect MoE routing to the broader literature on embedding inversion. We outline practical leakage scenarios (e.g., distributed inference and side channels) and show that adding noise reduces but does not eliminate reconstruction. Our findings suggest that expert selections in MoE deployments should be treated as sensitive as the underlying text.¹

1 INTRODUCTION

As modern large language models have grown in scale, there is growing demand for compute-efficient transformer architectures. Mixture-of-experts (MoE) models address this by activating only a subset of parameters per token, speeding up training and inference (Shazeer et al., 2017; Fedus et al., 2022; Jiang et al., 2024). Consequently, MoE architectures are widely used in modern LLMs. This motivates an examination of the expert-selection mechanism in these models. In this work, we show an attack that exploits MoE routing: the expert selections can leak enough information to reconstruct the underlying text.

2 RELATED WORK

Embedding inversion. A closely related line of work studies inversion of continuous text representations. Morris et al. (2023) propose *vec2text*, showing that a learned decoder can reconstruct text from sentence embeddings, demonstrating that embedding vectors can leak substantial lexical and semantic content; see also earlier analyses of embedding leakage (Song & Raghunathan, 2020). Zhang et al. (2025) propose *ZSInvert*, which targets black-box embedding APIs and performs universal, zero-shot inversion without training an embedding-specific decoder. Huang et al. (2024) study transferable embedding inversion, showing that an attacker can recover text from embeddings without querying the target embedding model. Our setting is different: expert selections are a *discrete* and lower-bandwidth intermediate signal than full embedding vectors or hidden states, but are emitted repeatedly across layers and tokens. We show that even these expert-selection traces can support high-fidelity reconstruction.

MoE side channels. Ding et al. (2025) show that MoE routing information can leak via architectural side channels (e.g., GPU performance counters), and demonstrate downstream prompt inference and response reconstruction using a logistic regression decoder and templated-prompt strategies. Our work complements this: we study the decoding problem given (possibly partial) expert-selection traces and show that sequence-level decoding can substantially improve reconstruction

¹Our dataset and code are available on  HuggingFace.

over per-token classifiers. As a stronger baseline than logistic regression, we use a 3-layer MLP decoder. We also describe additional leakage surfaces beyond the specific side-channel instantiations considered in MoEcho, such as distributed inference and pipeline-parallel MoE.

Model theft and extraction. Broader work on attacks against deployed language models studies extracting sensitive information or model components from production systems (Carlini et al., 2024), complementing our focus on privacy leakage from intermediate routing signals.

Output inversion and prompt extraction. Related work also studies reconstructing prompts from observable model outputs. Zhang et al. (2024) extract prompts by inverting LLM outputs, which is complementary to our setting where the observed signal is an internal routing trace rather than generated text.

3 THREAT MODEL

Observed signal. The adversary observes only the router’s expert selections for each token at one or more layers. The adversary may observe a subset of layers and does not observe router logits, router weights, hidden states, or expert outputs.

Goal. Given the set of selected experts corresponding to an unknown token sequence, the adversary aims to reconstruct the underlying text, ideally recovering a semantically similar sequence if not the exact tokens.

Auxiliary knowledge at attack time. We assume the adversary knows the tokenizer used by the victim model and the MoE routing configuration (e.g., the number of experts and k). In our experiments, we assume the model family and routing configuration match `gpt-oss-20b`.

Data access for learning-based decoders. For our MLP and sequence decoder, we assume the adversary can obtain training pairs of “(token, expert-selection trace)” from a same-family model, or from other sources that expose both text and expert-selection traces (e.g., internal logs in distributed inference). We trained the sequence decoder on contiguous token sequences (not shuffled tokens), preserving the natural order in which tokens (and therefore selected experts) appear.

4 ATTACK SURFACES

We now describe practical settings in which an adversary may obtain expert-selection traces. The key observation is that expert selections are a low-throughput signal, but they can be exposed whenever routing decisions cross boundaries (e.g., between devices, processes, or administrative domains) or leak through side channels. An adversary can collect “(text, trace)” pairs from benign workloads where text is known, train an inverter on these pairs, then apply the trained inverter to reconstruct text from traces of sensitive workloads.

Distributed inference. In distributed inference settings, a malicious host machine running a model (or a subset of its layers or experts) can observe full or partial routing traces and decode the original text, violating user privacy.

Physical side channels. In supply-chain or co-residency scenarios, attackers may be able to collect side channel measurements (e.g., via power draw or electromagnetic emissions) to infer which experts are selected at runtime, then map these routing traces to confidential tokens using our decoding method. Our experiments in this paper are focused on the latter half of this attack, assuming the adversary has already identified routing traces; prior work demonstrates that MoE routing can be inferred via architectural side channels (e.g., GPU performance counters) (Ding et al., 2025), suggesting that physical side channels are a plausible additional leakage route.

Pipeline-parallel MoE. If experts are sharded across data center nodes (common in pipeline-parallel MoE), an adversary might only need to detect which GPU exhibits activity over time, then infer the responsible experts via frequency analysis (or get expert identification for free when each expert uniquely maps to a single device).

5 DECODING ATTACK

We use OpenWebText for evaluation and training since it contains a wide variety of text, including high-entropy data like passwords and API keys. To obtain training data, we run `gpt-oss-20b` (32 experts, top-4 routing, 24 layers, vocab size 201,088) over 100M tokens of OpenWebText split into 32-token chunks in prefill (no autoregressive generation), yielding “(token sequence, expert-selection trace)” pairs. Here an *expert-selection trace* (also called a *routing trace*) consists of the router’s unordered top- k expert indices for each token at each observed layer. We use these terms interchangeably throughout. Top-1, top-5, and top-10 exact token decoding accuracies are evaluated on a held-out OpenWebText split (10M tokens) disjoint from training; unless otherwise stated, the trace includes expert selections from all 24 layers.

Model and notation. Let $x_{1:T} = (x_1, \dots, x_T)$ denote a token sequence of length T . For a model with L MoE layers, n experts per layer, and top- k routing, let ϕ be the (deterministic) routing trace function mapping a token sequence to the per-layer expert selections.

$$I = \phi(x_{1:T}), \quad (1)$$

$$I = (I_{\ell,t})_{\ell=1, t=1}^{L, T}, \quad (2)$$

$$I_{\ell,t} \subseteq \{1, \dots, n\}, \quad |I_{\ell,t}| = k. \quad (3)$$

Here $I_{\ell,t}$ is the *unordered* set of the k experts selected for token x_t at layer ℓ . The attacker observes I and aims to recover $x_{1:T}$.

For learning-based inversion, we train a decoder $p_\theta(x_{1:T} \mid I)$ by maximum likelihood, i.e., minimizing the negative log-likelihood over training pairs $(x_{1:T}, I)$.

Single-token MLP. A 3-layer MLP trained to predict a token from its expert selections obtains 63.1% top-1 accuracy (80.3% top-5, 84.3% top-10; Figure 1). This decoder treats each token independently, learning a mapping from a single token’s expert-selection trace to a distribution over the vocabulary. Ablations indicate that performance declines when the MLP has more than six layers.

Sequence decoder. We train an encoder-only transformer that maps the expert-selection trace to the token sequence. Unlike the MLP baseline, the transformer consumes the entire length- T expert-selection trace jointly and predicts the full token sequence, allowing it to exploit dependencies across positions. Our implementation first converts the per-layer top- k expert selections into 32-dimensional binary vectors with exactly 4 ones (to represent `gpt-oss-20b` with $n = 32, k = 4$), applies a small per-layer MLP and concatenates representations across the layers of the MoE model under observation, then projects into a token-level embedding stream with learned positional embeddings. We then apply a stack of non-causal self-attention blocks and predict token logits with a linear head, training with cross-entropy on the observed positions. This model achieves 91.2% top-1 accuracy (94.3% top-5, 94.8% top-10) on 10M held-out OpenWebText tokens when trained on traces from 100M tokens, substantially outperforming the MLP baseline. We observe that accuracy degrades gracefully with less training data (Figure 2); accuracy as a function of token frequency is shown in Figure 3.

6 INFORMATION LEAKAGE FROM EXPERT SELECTIONS

Router outputs for a token are conditioned on the context and therefore deterministic for a fixed prefix, up to floating-point error. In practice, near-ties in top- k , GPU nondeterminism, and quantization can cause occasional flips. Recent work argues that hidden states in decoder-only transformers are almost surely injective and hence invertible (Nikolaou et al., 2025). One might conjecture that router logits (as smooth images of these states) preserve token identity with high probability. However, quantization and floating-point errors can break strict invertibility, suggesting expert selections might not allow exact reconstruction.

Despite that, we empirically show that expert selections still provide ample information for decoding, while relaxing threat-model assumptions and enabling additional attack surfaces. For example, side-channel approaches such as MoEcho (Ding et al., 2025) use NVIDIA Performance Counters

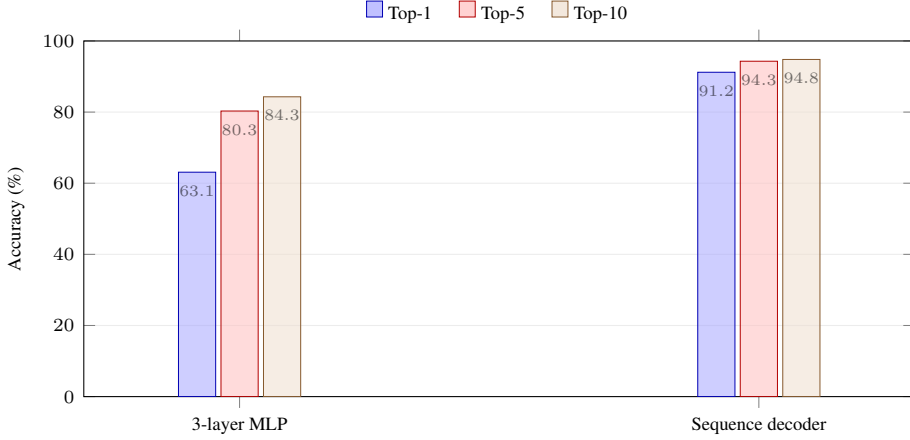


Figure 1: Accuracy of decoding tokens from expert selections on OpenWebText.

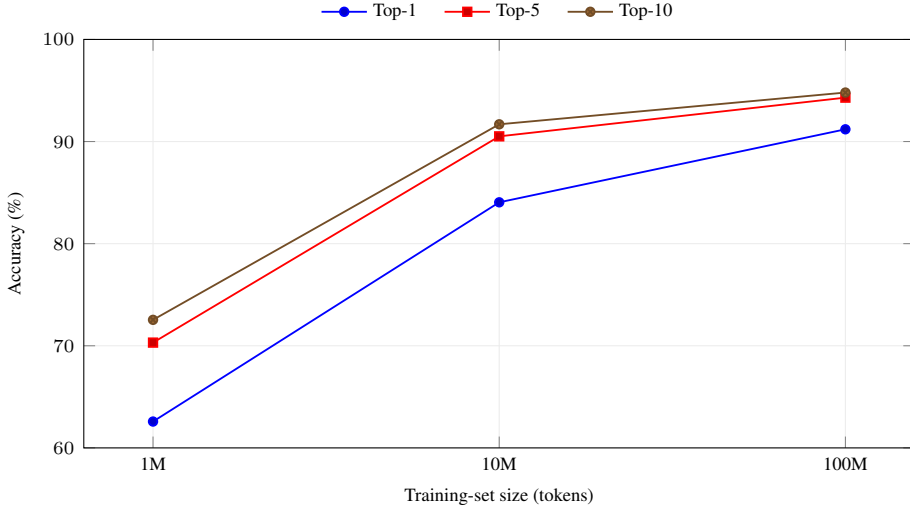


Figure 2: Accuracy vs. training-set size for the sequence decoder on OpenWebText.

to infer activated experts and decode those inferred expert selection traces into text using a logistic regression decoder. Conceptually, expert selections resemble discrete ‘‘embeddings’’ of tokens and contexts, connecting our setting to existing embedding inversion attacks (Morris et al., 2023).

We define *expert selections* at a layer as the unordered set of experts selected by top- k routing among n experts. Let I_ℓ denote this set at layer ℓ . For a single layer, the number of possible selections is $\binom{n}{k}$, so the entropy is bounded by

$$H(I_\ell) \leq \log_2 \binom{n}{k} \text{ bits,} \quad (4)$$

with equality only if selections are uniform over all $\binom{n}{k}$ outcomes.

Across L layers, let $I_{1:L} = (I_1, \dots, I_L)$ be the routing trace for a token. By subadditivity of entropy,

$$H(I_{1:L}) \leq \sum_{\ell=1}^L H(I_\ell) \leq L \log_2 \binom{n}{k}. \quad (5)$$

For gpt-oss-20b ($n = 32, k = 4$) with $L = 24$, this yields an (extremely loose) upper bound of $24 \log_2 \binom{32}{4} \approx 363$ bits per token.

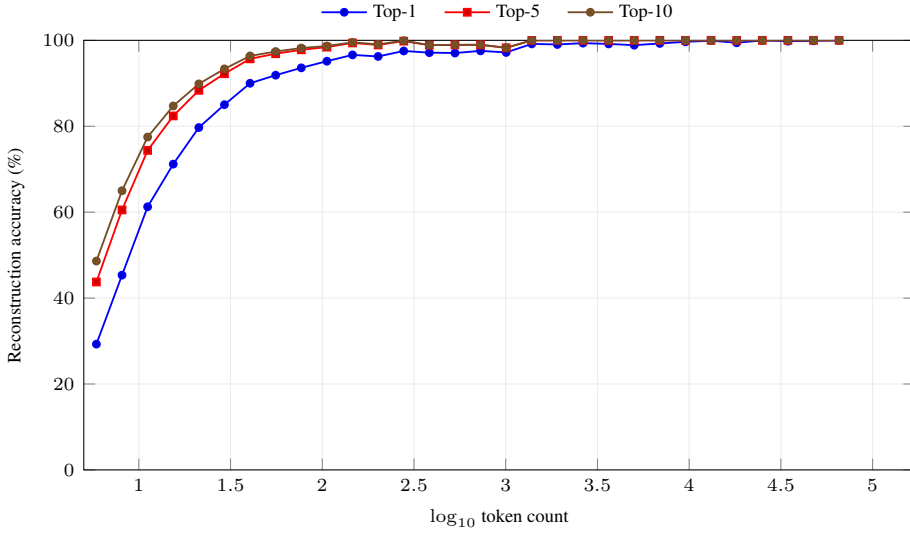


Figure 3: Accuracy vs. token frequency on a 2M slice of OpenWebText.

This value should not be read as “bits of token identity.” In practice, selections are correlated across layers and depend on context, so the effective entropy is substantially lower.

7 LAYERWISE INFORMATION ANALYSIS

Which layers are most informative? We estimate the layerwise entropy of expert selections and the mutual information between layers. Figure 4 visualizes the resulting entropy profile across the 24 layers, computed with plug-in estimators over empirical selection distributions. The sum of entropy across all layers is 206 bits, which is a tighter upper bound for the total router information content per token.

Random variables. Let t be a uniformly random token position in our trace dataset. For each MoE layer ℓ , define the routing random variable

$$I_\ell := I_{\ell,t}, \quad (6)$$

where $I_{\ell,t}$ is the *unordered* set of the top- k expert selections for token position t at layer ℓ .

Per-layer entropy estimation. Let $\hat{p}_\ell(S)$ be the fraction of token positions whose selection at layer ℓ equals expert set S . We estimate the entropy with the plug-in estimator

$$\hat{H}(I_\ell) = - \sum_{S \in \mathcal{S}_\ell} \hat{p}_\ell(S) \log_2 \hat{p}_\ell(S), \quad (7)$$

where \mathcal{S}_ℓ is the set of distinct expert sets observed at least once at layer ℓ (unobserved outcomes are treated as having probability 0). Given the large sample size, we expect finite-sample bias to be small for $\hat{H}(I_\ell)$.

Mutual information heatmap construction. We compute plug-in estimates of inter-layer mutual information to characterize redundancy in routing patterns across layers; we use these estimates primarily for qualitative comparison. Early layers (1-7) show high mutual information with each other, while middle layers (particularly around layer 11) show reduced mutual information with both early and late layers, suggesting distinct routing regimes.

For each pair of layers (i, j) with $i < j$, we accumulate empirical counts over observed pairs $(I_{i,t}, I_{j,t})$ across token positions, yielding an empirical joint distribution \hat{p}_{ij} and marginals \hat{p}_i, \hat{p}_j .

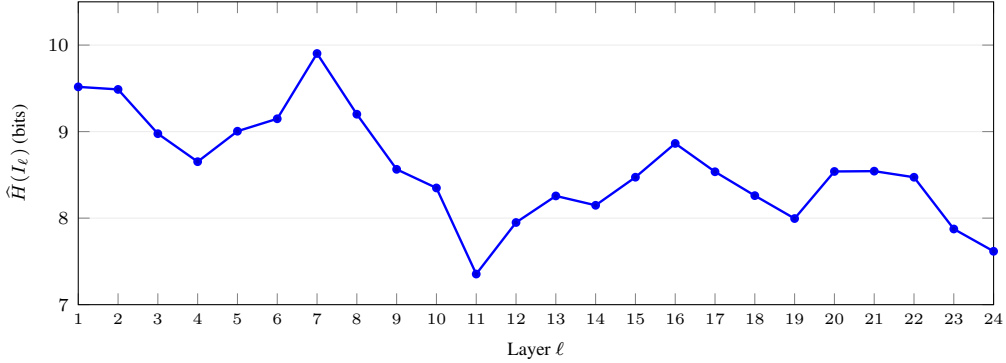


Figure 4: Estimated per-layer entropy of expert selections.

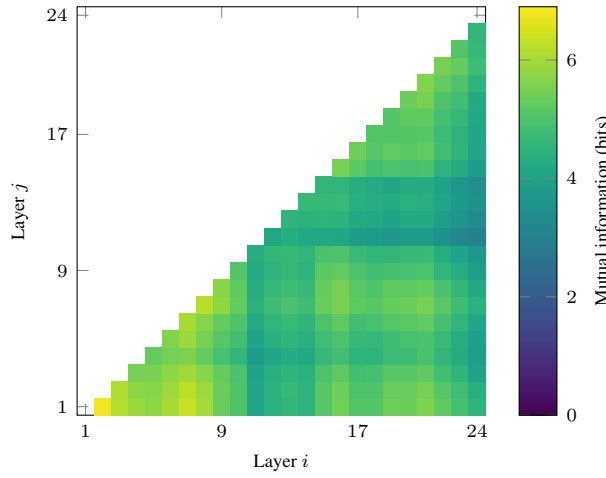


Figure 5: Estimated mutual information between layers' expert selections.

We then compute the plug-in mutual information estimator

$$\widehat{I}(I_i; I_j) = \sum_{(a,b) \in \mathcal{P}_{ij}} \hat{p}_{ij}(a,b) \log_2 \left(\frac{\hat{p}_{ij}(a,b)}{\hat{p}_i(a) \hat{p}_j(b)} \right), \quad (8)$$

where \mathcal{P}_{ij} ranges over expert-set pairs observed at least once (unobserved pairs are treated as having probability 0).

8 MITIGATIONS

Because our attack assumes access to expert selections, the most direct mitigation is to treat expert-selection traces as sensitive outputs and minimize their exposure. Concretely, production deployments should avoid returning, logging, or exporting per-token expert selections unless also handling tokens the same way. Production deployments should treat routing information as though it is the same as tokens, especially when such information crosses trust boundaries between tenants, machines, or administrative domains.

Expert-noise robustness. To simulate measurement error and probabilistic or imperfect mitigations, we evaluate robustness to expert-selection trace noise by independently corrupting a fraction p of the observed expert selections by replacing them with a uniformly random expert, and report top- k token recovery accuracy as a function of p (Figure 6).

For settings where expert selections may leak through side channels (Ding et al., 2025), we view several engineering mitigations as reasonable: (i) reduce the distinguishability of expert execution by

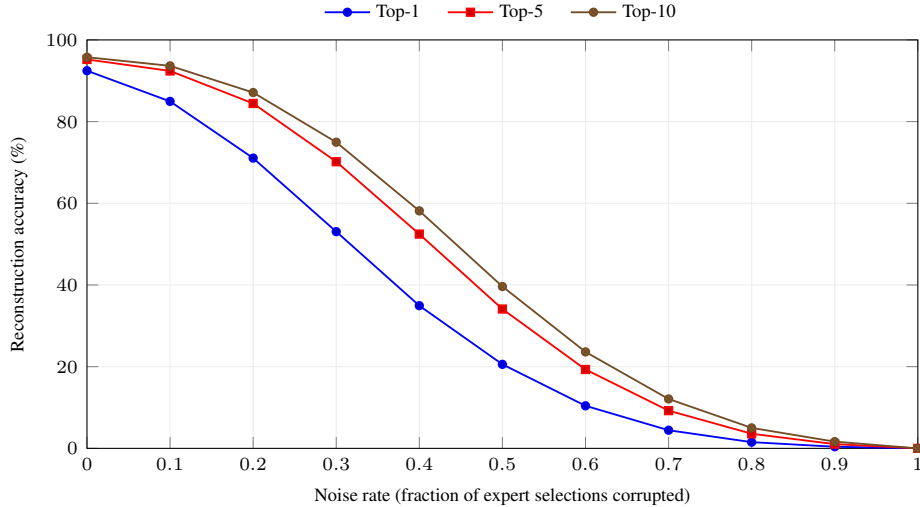


Figure 6: Expert-selection noise vs. reconstruction accuracy on OpenWebText.

balancing expert workloads and memory access patterns; (ii) add dummy compute or constant-work padding to blur expert-dependent activity; (iii) introduce randomness in routing (e.g., logit noise) or periodically permute expert identity to reduce trace stability; (iv) harden the routing/expert execution boundary (e.g., isolate co-resident workloads or disable exposure of fine-grained performance counters); and (v) make physical side channel measurements more difficult by shielding against leakage and removing or securing nearby sensors.

These defenses may incur performance or quality costs (e.g., increased compute or perturbed routing decisions); we leave a quantitative evaluation of the tradeoffs to future work.

9 LIMITATIONS

Scalability to long sequences. Our strongest results are for short sequences (32 tokens), and while the sequence decoder can recover useful information for longer windows, we have not systematically characterized the limits of inversion as sequence length grows (e.g., hundreds or thousands of tokens). Longer contexts increase ambiguity and may require more expressive architectures or search procedures.

Access and transferability. Our threat model assumes an adversary can obtain expert-selection traces and a compatible tokenizer, and that the adversary can collect sufficient “(text, expert-selection trace)” training pairs for a learning-based inverter (e.g., via an instrumented model instance, a same-family model, or internal logs). In practice, transfer to different model families, tokenizers, routing configurations, or expert permutations may reduce reconstruction quality; we do not evaluate cross-model transfer.

Partial traces. Although our threat model allows observing only a subset of layers, our main evaluations assume expert selections from all 24 layers. We evaluated information content per layer but have not measured reconstruction accuracy with such partial information since that requires retraining the model.

Decoder complexity. Our sequence decoder uses a learned encoder-only transformer and benefits from large-scale training data. More sophisticated decoding procedures (e.g., beam search or iterative refinement on top of the decoder) may further improve reconstruction, but we leave such extensions to future work.

ACKNOWLEDGMENTS

This work was supported by  MATS and  SPAR. Various contributions were made by Jacob Lagerros, Natalia Kokoromyti, Luc Chartier, George Tourtellot and Krystal Maughan.

ETHICS STATEMENT

This work studies privacy leakage mechanisms in MoE language model deployments. While it can inform defensive engineering (e.g., treating routing traces as sensitive outputs and hardening against side channels), it also could be misused to recover private user prompts when routing signals leak. We therefore emphasize mitigations and recommend minimizing exposure of routing traces and considering side-channel-resilient deployment practices for MoE inference. OpenWebText contains sensitive data; however, the original text is tokenized and isn't explicitly stored. By omitting details of methods to extract expert identities from side channel measurements, this work primarily advances the theoretical understanding of this type of attack rather than providing a practical method to breach confidentiality in real-world deployments.

REFERENCES

Nicholas Carlini, Daniel Paleka, Krishnamurthy Dj Dvijotham, Thomas Steinke, Jonathan Hayase, A. Feder Cooper, Katherine Lee, Matthew Jagielski, Milad Nasr, Arthur Conmy, Eric Wallace, David Rolnick, and Florian Tramèr. Stealing part of a production language model. In *Proceedings of the 41st International Conference on Machine Learning*, volume 235 of *Proceedings of Machine Learning Research*, pp. 5680–5705. PMLR, 2024. URL <https://proceedings.mlr.press/v235/carlini24a.html>.

Ruyi Ding, Tianhong Xu, Xinyi Shen, Aidong Adam Ding, and Yunsi Fei. Moecho: Exploiting side-channel attacks to compromise user privacy in mixture-of-experts LLMs, 2025. URL <https://arxiv.org/abs/2508.15036>.

William Fedus, Barret Zoph, and Noam Shazeer. Switch transformers: Scaling to trillion parameter models with simple and efficient sparsity. *Journal of Machine Learning Research*, 23(120):1–39, 2022. URL <https://jmlr.org/papers/v23/21-0998.html>.

Yu-Hsiang Huang, Yuche Tsai, Hsiang Hsiao, Hong-Yi Lin, and Shou-De Lin. Transferable embedding inversion attack: Uncovering privacy risks in text embeddings without model queries. In Lun-Wei Ku, Andre Martins, and Vivek Srikumar (eds.), *Proceedings of the 62nd Annual Meeting of the Association for Computational Linguistics (Volume 1: Long Papers)*, pp. 4193–4205, Bangkok, Thailand, August 2024. Association for Computational Linguistics. doi: 10.18653/v1/2024.acl-long.230. URL <https://aclanthology.org/2024.acl-long.230/>.

Albert Q. Jiang, Alexandre Sablayrolles, Antoine Roux, Arthur Mensch, Blanche Savary, Chris Bamford, Devendra Singh Chaplot, Diego de las Casas, Emma Bou Hanna, Florian Bressand, Gianna Lengyel, Guillaume Bour, Guillaume Lample, Lélio Renard Lavaud, Lucile Saulnier, Marie-Anne Lachaux, Pierre Stock, Sandeep Subramanian, Sophia Yang, Szymon Antoniak, Teven Le Scao, Théophile Gervet, Thibaut Lavril, Thomas Wang, Timothée Lacroix, and William El Sayed. Mixtral of experts, 2024. URL <https://arxiv.org/abs/2401.04088>.

John Morris, Volodymyr Kuleshov, Vitaly Shmatikov, and Alexander Rush. Text embeddings reveal (almost) as much as text. In Houda Bouamor, Juan Pino, and Kalika Bali (eds.), *Proceedings of the 2023 Conference on Empirical Methods in Natural Language Processing*, pp. 12448–12460, Singapore, December 2023. Association for Computational Linguistics. doi: 10.18653/v1/2023.emnlp-main.765. URL <https://aclanthology.org/2023.emnlp-main.765/>.

Giorgos Nikolaou, Tommaso Mencattini, Donato Crisostomi, Andrea Santilli, Yannis Panagakis, and Emanuele Rodolà. Language models are injective and hence invertible, 2025. URL <https://arxiv.org/abs/2510.15511>.

Noam Shazeer, Azalia Mirhoseini, Krzysztof Maziarz, Andy Davis, Quoc Le, Geoffrey Hinton, and Jeff Dean. Outrageously large neural networks: The sparsely-gated mixture-of-experts layer. In

International Conference on Learning Representations, 2017. URL <https://arxiv.org/abs/1701.06538>.

Congzheng Song and Ananth Raghunathan. Information leakage in embedding models, 2020. URL <https://arxiv.org/abs/2004.00053>.

Collin Zhang, John Xavier Morris, and Vitaly Shmatikov. Extracting prompts by inverting LLM outputs. In Yaser Al-Onaizan, Mohit Bansal, and Yun-Nung Chen (eds.), *Proceedings of the 2024 Conference on Empirical Methods in Natural Language Processing*, pp. 14753–14777, Miami, Florida, USA, November 2024. Association for Computational Linguistics. doi: 10.18653/v1/2024.emnlp-main.819. URL <https://aclanthology.org/2024.emnlp-main.819/>.

Collin Zhang, John X. Morris, and Vitaly Shmatikov. Universal zero-shot embedding inversion, 2025. URL <https://arxiv.org/abs/2504.00147>.

A APPENDIX

A.1 MOE ROUTER MECHANISM

We briefly describe standard top- k routing used in many MoE transformers. In OpenAI’s reference implementation of `gpt-oss-20b`, routing occurs in the MoE MLP sublayer: given the MLP input vector $x \in \mathbb{R}^d$ (i.e., the residual stream entering the MoE MLP, after the attention sublayer), routing proceeds as follows:

1. **Normalize.**

$$h = \text{RMSNorm}(x). \quad (9)$$

2. **Score each expert.** Compute logits over experts with a single affine map (where n is the number of experts):

$$s = W_r h + b \in \mathbb{R}^n. \quad (10)$$

We refer to s as the *expert logits*.

3. **Pick the experts.** Select indices of the top- k experts:

$$I = \text{TopK}(s, k). \quad (11)$$

We call I the *expert selections*.

4. **Compute mixing weights.** Convert scores to nonnegative weights and normalize across the selected experts (e.g., using a softmax over s_I):

$$\alpha = \text{softmax}(s_I). \quad (12)$$

5. **Run selected experts.** Each selected expert e_i processes h (e.g., a SwiGLU MLP) to produce

$$y_i = e_i(h). \quad (13)$$

6. **Combine.** Take the weighted sum:

$$y = \sum_{i \in I} \alpha_i y_i. \quad (14)$$

7. **Residual add.** Return $x + y$ to the residual stream.

In simple terms, each token gets a score for each expert (via a learned gate matrix and bias), is routed through the k most preferred experts, and the resulting expert outputs are mixed and added back to the residual stream. In our main setting, OpenAI’s `gpt-oss-20b` has 24 layers, 32 experts per layer, and routes top-4 experts per token.